

# Adaptive altitude flight control of quadcopter under ground effect and time-varying load: theory and experiments

Ji-Won Lee<sup>1,\*</sup> , Nguyen Xuan-Mung<sup>2,\*</sup> , Ngoc Phi Nguyen<sup>2</sup>, and Sung Kyung Hong<sup>2</sup>

Journal of Vibration and Control  
2023, Vol. 29(3-4) 571–581

© The Author(s) 2021



Article reuse guidelines:

[sagepub.com/journals-permissions](https://sagepub.com/journals-permissions)

DOI: 10.1177/10775463211050169

[journals.sagepub.com/home/jvc](https://journals.sagepub.com/home/jvc)



## Abstract

In recent years, the boom of the quadcopter industry resulted in a broad range of real-world applications which highlighted the urgent need to improve quadcopter control quality. Typically, external disturbances, such as wind, parameter uncertainties caused by payload variations, or the ground effect, can severely degrade the quadcopter's altitude control performance. Meanwhile, widely used controllers like the proportional-integral-derivative control cannot guarantee control performance when the system is critically affected by factors that exhibit a high degree of variability with time. In this paper, an adaptive control algorithm is proposed to improve quadcopter altitude tracking performance in the presence of both the ground effect and a time-varying payload. First, we derive an adaptive altitude control algorithm using the sliding mode control technique to account for these uncertainties in the quadcopter dynamics model. Second, we apply Lyapunov theory to analyze the stability of the closed-loop system. Finally, we conduct several numerical simulations and experiments to validate the effectiveness of the proposed method.

## Keywords

Adaptive control, sliding mode, quadcopter, altitude flight, ground effect, time-varying payload

## 1. Introduction

In recent years, unmanned aerial vehicles (UAVs) have become increasingly popular in many sectors, including military, surveillance, inspection, agriculture, and transportation (Alexis et al., 2009; Goodarzi et al., 2015; Elmokadem, 2019; Rodriguez-Mata et al., 2018). Quadcopters, one type of UAV, have been attracting a great deal of attention from scientists due to their numerous advantages such as economic efficiency, high maneuverability, and convenient maintenance. Most quadcopter applications require a reliable altitude tracking controller. However, the design of a stable and high-performance quadcopter tracking controller often faces several difficulties related to nonlinearities and coupled-control-input problems due to the system being underactuated (Hua et al., 2009; Zhang et al., 2014).

To address these issues, several control methods have been investigated. The backstepping approach has been introduced as an effective control scheme for underactuated systems (Das et al., 2009; Ramirez-Rodriguez et al., 2014; Xuan-Mung and Hong, 2019). Dong et al. (2014), Jia et al. (2017), and Zhang et al. (2018) presented various control methods to minimize trajectory tracking errors when external disturbances were introduced. Many advanced algorithms

based on sliding mode control (SMC) techniques have been proposed to compensate for system model uncertainties (Besnard et al., 2012; Muñoz et al., 2017; Nguyen and Hong 2019). However, despite having certain advantages, the aforementioned model-based control methods either require considerable computational resources or complicated gain-tuning processes. In contrast, the proportional-integral-derivative (PID) control technique, used in many practical applications, is known to be a simple and efficient method to satisfy many control requirements.

<sup>1</sup>Human-Robot Interaction Research Center, Korea Institute of Robotics and Technology Convergence, Pohang, South Korea

<sup>2</sup>Faculty of Mechanical and Aerospace Engineering, Sejong University, Seoul, South Korea

Received: 15 March 2021; revised: 20 July 2021; accepted: 6 September 2021

\*These authors contributed equally to this work

### Corresponding author:

Sung Kyung Hong, Department of Aerospace Engineering, and Convergence Engineering for Intelligent Drone, Sejong University, Gwangjin-gu, Seoul 05006, South Korea.

Email: [skhong@sejong.ac.kr](mailto:skhong@sejong.ac.kr)

To keep pace with the great advances in technology, quadcopter control techniques also must improve to meet the strict safety criteria of new applications in fields such as precision agriculture, cargo transportation, and fire-fighting. A common problem faced by all these applications is that a varying mass of the system will always lead to a degradation in altitude control performance and will inevitably expose the limitations in some PID controllers' adaptiveness and robustness. An additional problem in the field of aerial vehicle control is the variation of system parameters, especially when fuel represents a significant portion of the total mass of the vehicle as is the case in rockets and satellites for instance (Cho et al., 2020; Gao and Wang, 2013; Rubio Hervas and Reyhanoglu, 2014). Furthermore, while the mass variation raises altitude control design issues, the ground effect is an additional problem that needs to be considered (Danjun et al., 2015; Sanchez-Cuevas et al., 2017). In general, the impact of the ground effect has often been neglected in altitude control. However, from a practical perspective, quadcopters are often used for flights close to low-altitude surfaces where the ground effect can considerably reduce the control performance. Therefore, finding a controller that can cope with both the variation in system parameters and the ground effect has become a pressing issue not only when it comes to quadcopter controls but also for other UAV systems.

To that end, various control approaches have been proposed in the literature employing different techniques. In a paper by Qiao et al. (2018), a gain-scheduled PID controller was applied to a quadcopter system to achieve a payload drop task. Simulation results were shown to demonstrate the effectiveness of this approach. This method has also been used in several other studies (Sadeghzadeh et al., 2014; Wei et al., 2014) as it inherited the simplicity from conventional PID controllers but was able to exhibit a certain capability to deal with system parameter changes. However, as the gains had been chosen from a predefined series, this method usually exhibits certain drawbacks when it comes to system stability analysis. Other approaches using neural networks were investigated by Lee et al. (2015) and Sierra and Santos (2019). Through numerical simulations, they were able to demonstrate that these intelligent control strategies could learn to adapt to changing conditions. However, their high computational cost excludes them from a wide range of applications that require small, low-cost UAV systems. An additional weakness of this neural network-based approach is that the systems' stability is inherently difficult to evaluate. The linear parameter varying (LPV) control technique (Pham et al., 2019) is capable to overcome this disadvantage and has seen increasing use. However, LPV controllers are also known to require considerable computational resources. Other control approaches have been tested with regard to their ability to cope with variations in the vertical dynamics of quadcopters, including a switched adaptive control (Sankaranarayanan and Roy,

2018) and an adaptive prescribed performance control (Hua et al., 2018). However, the applicability of these approaches was never tested experimentally. Meanwhile, the SMC technique has become a popular choice in controlling systems that need to be robust against external disturbances and parameter uncertainties (Lee et al., 2009). In the study by Liu et al. (2019), a learning rate-based SMC was applied to a variable load quadcopter. While the authors successfully demonstrated the robustness of their algorithm through experiments, they did not consider (dynamically) the influence of the ground effect in low-altitude flights and did not present any demonstrations of such scenarios.

In this paper, we propose an adaptive sliding mode controller (ASMC) to achieve the goal of altitude tracking control in the presence of considerable system parameter variations and the ground effect. The main contributions of this study are fourfold:

- (i) To account for uncertainty, we introduce an unknown time-varying parameter to the quadcopter's dynamic model that will be estimated by our adaptation law. Using the obtained dynamics model and Lyapunov theory, we design an adaptive sliding mode control law and mathematically prove its stability. To improve the system control performance, it is crucial to find a suitable adaptation law that provides reliable estimates of the uncertainties.
- (ii) Compared to conventional and commonly used PID controllers, our controller delivers a significantly improved performance with regard to both settling time and robustness against the varying terms.
- (iii) Unlike most existing studies on adaptive quadcopter altitude control (see above) that exclusively tested and verified their algorithms via numerical simulations, we conducted both simulations and experiments of actual flight conditions to demonstrate the effectiveness of our method.
- (iv) During the experiments, we utilized a water discharge system consisting of a plastic container (to serve as a water tank), a water pump, and an Arduino control board (to control the pump automatically). This approach was intended to add realism to our experiments and bring them closer to real-world applications, such as unmanned aerial firefighters, agricultural spraying drones, or urban air mobility.

The remainder of this paper is organized as follows. Section 2 presents the dynamics of the quadcopter with the ground effect taken into account. In Section 3, the sliding mode controller and adaptation law are derived, and the stability of the closed-loop system is proved using Lyapunov theory. The simulation and experimental results are discussed in Section 4 before ending with the conclusions in Section 5.

## 2. Quadcopter dynamics model and problem formulation

In this section, we briefly present the quadcopter dynamics model, which has already been investigated in several previous studies (Kim et al., 2009; Mahony et al., 2012; Xuan-Mung et al., 2020).

Let  $\phi$ ,  $\theta$ , and  $\psi$  be the angles representing the vehicle attitude, that is, roll, pitch, and yaw, respectively, where  $|\phi| < \pi/2$ ,  $|\theta| < \pi/2$ , and  $|\psi| \leq \pi$ . Let  $x, y$ , and  $z$ , respectively, denote the quadcopter position along the  $x, y$ , and  $z$  axes in an inertial frame  $\{O_I\}$ .  $I_{xx}, I_{yy}$ , and  $I_{zz}$  are the inertial moments along the  $x, y$ , and  $z$  axes, respectively;  $m$  and  $l$  are the vehicle's total mass and arm length, respectively, and  $g$  is the gravitational acceleration. In this paper, the total mass  $m$  of the vehicle, including vehicle mass and its payload, is considered time-varying due to the variation of the payload in some ways. Besides, in order to address the ground effect, we take it into consideration in the vertical translational dynamics of the vehicle (Danjun et al., 2015).

We take it into consideration in the vertical translational dynamics of the vehicle (Danjun et al., 2015). Then, the quadcopter dynamics model can be described as follows

$$\begin{cases} \ddot{\phi} = \left( \frac{I_{yy} - I_{zz}}{I_{xx}} \right) \dot{\theta} \dot{\psi} + \frac{l}{I_{xx}} u_2 \\ \ddot{\theta} = \left( \frac{I_{zz} - I_{xx}}{I_{yy}} \right) \dot{\phi} \dot{\psi} + \frac{l}{I_{yy}} u_3 \\ \ddot{\psi} = \left( \frac{I_{xx} - I_{yy}}{I_{zz}} \right) \dot{\phi} \dot{\theta} + \frac{l}{I_{zz}} u_4 \\ \ddot{x} = (\cos \phi \sin \theta \cos \psi + \sin \phi \sin \psi) \frac{u_1}{m} \\ \ddot{y} = (\cos \phi \sin \theta \sin \psi - \sin \phi \cos \psi) \frac{u_1}{m} \\ \ddot{z} = \frac{\sigma}{m} \cos \phi \cos \theta u_1 - g \end{cases} \quad (1)$$

where

$$\begin{cases} u_1 = T_1 + T_3 + T_2 + T_4 \\ u_2 = l(T_2 - T_4) \\ u_3 = l(T_3 - T_1) \\ u_4 = c_d l(-T_1 - T_3 + T_2 + T_4) \end{cases} \quad (2)$$

with  $T_i = c_i \omega_i^2$  being the lift force generated by the motor  $i$  (Figure 1);  $\omega_i$  the motor speed;  $c_d$  and  $c_i$  the drag and thrust coefficients; and  $\sigma > 1$  being defined as

$$\sigma = \frac{1}{(1 - \rho R^2 / (4z_r)^2)} \quad (3)$$

where  $\rho$  is a surface coefficient of the ground effect,  $R$  the radius of the propellers, and  $z_r$  the vertical distance from the rotor to the ground.

Since both  $m$  and  $\sigma$  are uncertain terms, and for the sake of simplicity, let us define a variable  $\varsigma$  as

$$\varsigma = \frac{m}{\sigma} \quad (4)$$

The last equation in (1) can be rewritten using the control input  $u_1$  of the inertial frame as

$$\ddot{z} = \frac{1}{\varsigma} (\cos \phi \cos \theta) u_1 - g \quad (5)$$

Now, it is seen that both  $\sigma$  and  $m$  in (1) are positive time-varying and that these terms are coupled with the control input  $u_1$  that makes the control design task more taxing. The effort of this paper is to find out the adaptive control algorithm to drive the vehicle to achieve any given altitude setpoint,  $z_d$ , despite the variation of the aforementioned parameters.

## 3. Controller design

In this section, we present an adaptive altitude control algorithm for the quadcopter based on the SMC technique.

Let  $z_d$  be the desired altitude, and then the altitude tracking error can be computed as

$$e = z_d - z \quad (6)$$

and the sliding surface is formulated as

$$s = \dot{e} + k_1 e \quad (7)$$

with  $k_1$  being a positive constant to be chosen later.

Substituting (5) into the derivative of (7) yields

$$\dot{s} = \ddot{e} + k_1 \dot{e} = \ddot{z}_d - \left( \frac{1}{\varsigma} (\cos \phi \cos \theta) u_1 - g \right) + k_1 \dot{e} \quad (8)$$

Let  $\hat{\varsigma}$  denote the estimate of  $\varsigma$ .

**Theorem 1.** For any given altitude setpoint,  $z_d$ , the quadcopter system (1) is stable if the following holds:

(i) The estimate of  $\varsigma$ , that is,  $\hat{\varsigma}$ , is updated as

$$\dot{\hat{\varsigma}} = k_a s \left( \ddot{z}_d + g + k_1 \dot{e} + k_2 \text{sgn}(s) \right) \quad (9)$$

where  $k_2, k_a \in \mathbb{R}^+$ .

(ii) The control law is designed as

$$u_1 = \frac{\hat{\varsigma}}{\cos \phi \cos \theta} \left( \ddot{z}_d + g + k_1 \dot{e} + k_2 \text{sgn}(s) \right) \quad (10)$$

**Proof.** Let  $\tilde{\varsigma}$  represent the estimation error

$$\tilde{\varsigma} = \varsigma - \hat{\varsigma} \quad (11)$$

A Lyapunov function candidate,  $V$ , is introduced as

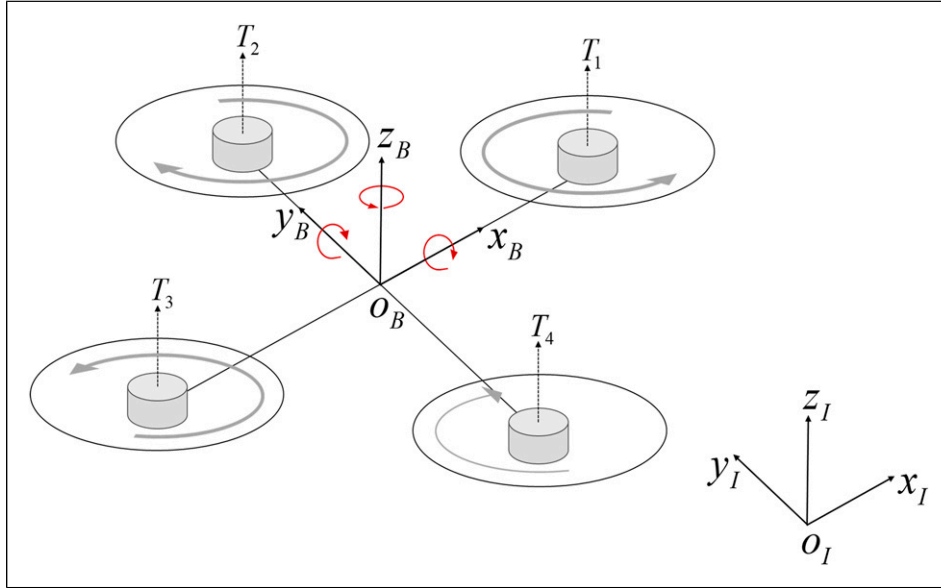


Figure 1. Configuration of the quadcopter.

$$V = \frac{1}{2}s^2 + \frac{\tilde{\zeta}^2}{2k_a\zeta} \quad (12)$$

Here, it is worth noting that from a practical point of view, the system mass and ground effect are not fast-varying quantities. Hence, we assume that  $\zeta$  varies slowly, that is,  $\dot{\zeta} \approx 0$ . Thus, the time derivative of  $V$  becomes

$$\dot{V} = s\dot{s} + \frac{2\tilde{\zeta}\dot{\zeta}\zeta - \tilde{\zeta}^2\dot{\zeta}}{2k_a\zeta^2} = s\dot{s} + \frac{\tilde{\zeta}\dot{\zeta}}{k_a\zeta} \quad (13)$$

Substituting (10) into (8), the derivative of the sliding surface becomes

$$\begin{aligned} \dot{s} = \ddot{z}_d - \left( -g + \frac{\hat{\zeta}}{\zeta \cos \phi \cos \theta} \left( \ddot{z}_d + k_1\dot{e} + g + k_2\text{sgn}(s) \right) \right) \\ + k_1\dot{e} = \frac{\tilde{\zeta}}{\zeta \cos \phi \cos \theta} \left( \ddot{z}_d + g + k_1\dot{e} + k_2\text{sgn}(s) \right) \\ - k_2\text{sgn}(s) \end{aligned} \quad (14)$$

From (9), (13), and (14), the time derivative of  $V$  is derived as

$$\begin{aligned} \dot{V} = \frac{\tilde{\zeta}}{\zeta \cos \phi \cos \theta} \left[ s \left( \ddot{z}_d + g + k_1\dot{e} + k_2\text{sgn}(s) \right) - \frac{\dot{\zeta}}{k_a} \right] \\ - k_2|s| = -k_2|s| < 0, \forall s \neq 0 \end{aligned} \quad (15)$$

From (15), it is clear that the system is stable. This completes the proof.

Table 1. Parameters of the experimental quadcopter platform.

Parameters	Values	Units
$m$	2.6 ~ 3.8	kg
$l$	0.225	m
$I$	[0.02 0.02 0.04]	kg · m <sup>2</sup>
$R$	0.1397	m
$\rho$	8.6	-

**Remark 1.** In practical applications, to eliminate the chattering phenomenon of the proposed controller, the signum functions (sgn) in equations (9) and (10) can be replaced by hyperbolic tangent functions (tanh) (Hassan, 2002), where  $\tanh(x) = (e^x - e^{-x}) / (e^x + e^{-x})$ .

**Remark 2.** The positive constant  $k_a$  is the adaptive gain and determines the adaptation speed, that is, the estimated value  $\hat{\zeta}$  converges faster to its actual value  $\zeta$  as  $k_a$  increases. However, a large  $\hat{\zeta}$  can cause significant system jerks when the mass varies considerably; it is therefore important to find a good balance between fast adaptation speed and keeping system jerks at an acceptable level.

**Remark 3.** The larger  $k_1$ , the faster the altitude error converges to zero. However, care must be taken when choosing  $k_1$  as large values can induce jerks and vibrations. Furthermore, the convergence speed of  $s$  is proportional to  $k_2$ . In our experiments, we found that  $k_1$  can range from 0.6 to 1.2, while  $k_2$  can be about 10 times larger than  $k_1$ . However, these ranges may depend on the type of quadcopter system and need to be tuned carefully by evaluating the system performance.



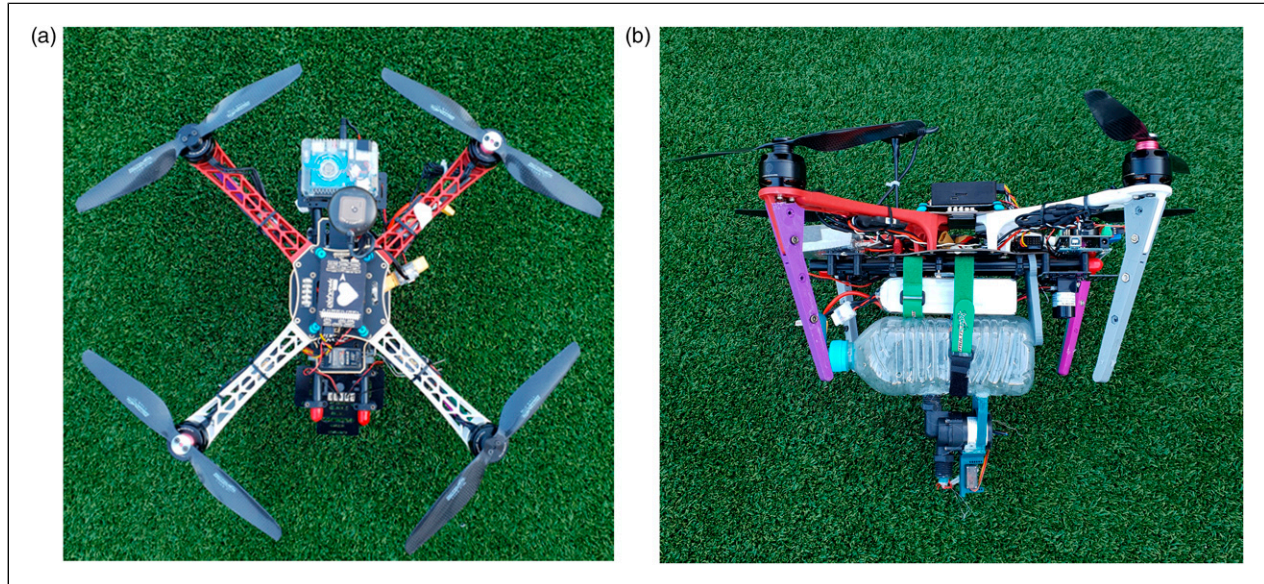


**Figure 2.** Top view (a) and side view (b) of the experimental quadcopter equipped with a mass-varying mechanism.



**Figure 3.** Scheme illustrating the communication between the avionics devices.

## 4. Simulation, experimental results, and discussions

### 4.1. Experimental setup

We used the DJI F450 quadcopter frame as our experimental platform (Table 1, Figure 2). The quadcopter consists of an inertial measurement unit (IMU) that provides information about the vehicle's attitude and acceleration, a global positioning system (GPS) receiver module to determine the position and velocity, a LidarLite V3 laser ranging sensor to measure the altitude, a Pixhawk flight control unit (FCU), and an Odroid companion computer. Additionally, a mass-varying mechanism (Figure 2(b)) was added to be able to simulate the mass variations that occur in some real-world systems, for example, in pesticide-spraying, fire-fighting, and delivery quadcopters. It consists of a water container with a capacity of 1 L and a pump that can discharge water at a constant rate of about 0.1 L/s, corresponding to a mass variation rate of 0.1 kg/s. The pump is automatically operated by an Arduino, which communicates with Odroid through the Rosserial protocol.

**Table 2.** Controller gains and initial state variables.

Parameters	Values
$k_d$	1
$k_1$	0.83
$k_2$	11.5
$k_{P\_outer}$	0.81
$[k_p \ k_i \ k_d]$	$[18.6 \ 10.8 \ 1]$
$[\phi_0 \ \theta_0 \ \psi_0]$	$[0 \ 0 \ 0]$
$[x_0 \ y_0 \ z_0]$	$[0 \ 0 \ 0]$

The Odroid computer and Pixhawk FCU exchange data with each other via Mavlink protocol (Figure 3).

Our proposed ASMC was implemented in the Odroid computer as a high-level controller, while the Pixhawk FCU operates the vehicle's stabilized controller.

The proposed algorithm is implemented in Odroid and operated at a frequency of 200 Hz (corresponding to a time sample of 0.005 s), and the controller gains are the same as in simulation (Table 2).

## 4.2. Simulation results and discussions

To highlight the effectiveness of our controller, we compare its altitude control performance with that of a conventional PID controller that is widely applied in a number of UAVs. The quadcopter parameters were fed into the mathematical model used for the numerical simulations. The final values for the controller gains were determined from simulations applying a trial-and-error approach (Table 2). The PID controller gains were found using the root-locus method. Two scenarios were simulated to provide information about the impacts of mass variation and ground effect and to improve the control performance of our new approach. As the ground effect only comes into play when the vehicle is flying low, we chose an altitude setpoint  $<1.5$  m for both scenarios.

**4.2.1. Altitude tracking flight under mass variation and no ground effect.** In this simulation scenario, we assumed no ground effect, that is,  $\sigma = 1$  and  $\zeta = m$ . In order to evaluate the control performance under different flight conditions, we examined two flight phases: (1) the system mass remains at its nominal value (2.6 kg) and (2) the system mass varies (Figure 4(a)). In Phase 1, the gains for our ASMC and the conventional PID controller are tuned to obtain similar system transient responses and settling times for both controllers while using step commands during the first 20 s. After receiving the commanded step of 1 m, both controllers produced the same result and the vehicle reached the desired altitude after 4.7 s (Figure 4(a)).

Phase 2 begins at  $t = 20$  s with the command to ascend with its 1.2 kg payload to 1.5 m. Compared to Phase 1, the PID now lags behind our ASMC as it takes the PID

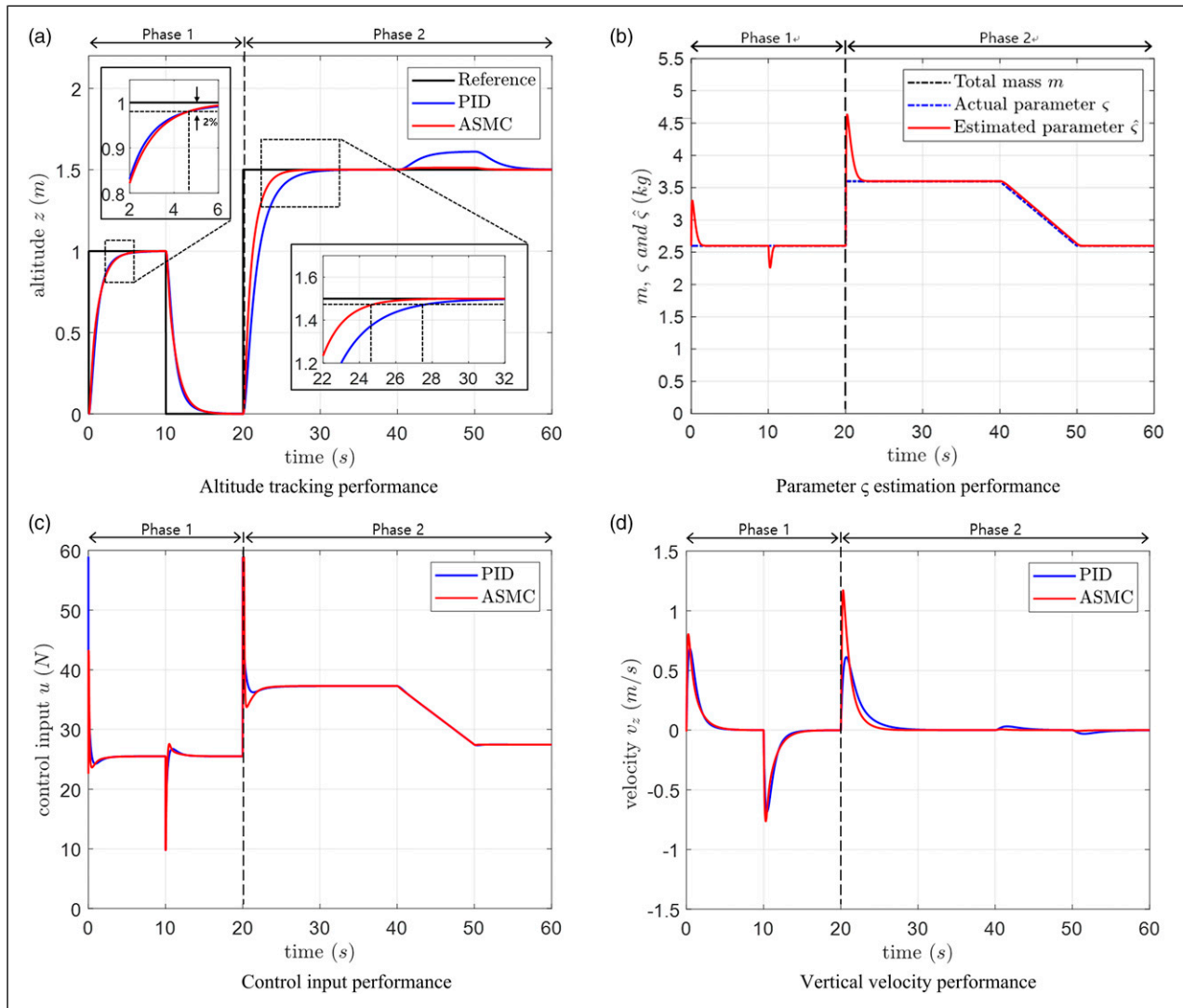


**Figure 4.** Performance comparisons for the scenario with the system mass variation only (no ground effect) between our controller (ASMC) and a conventional PID controller (PID). (a) Altitude tracking performance; (b) parameter  $\zeta$  estimation performance; (c) control input performance; (d) Vertical velocity performance.

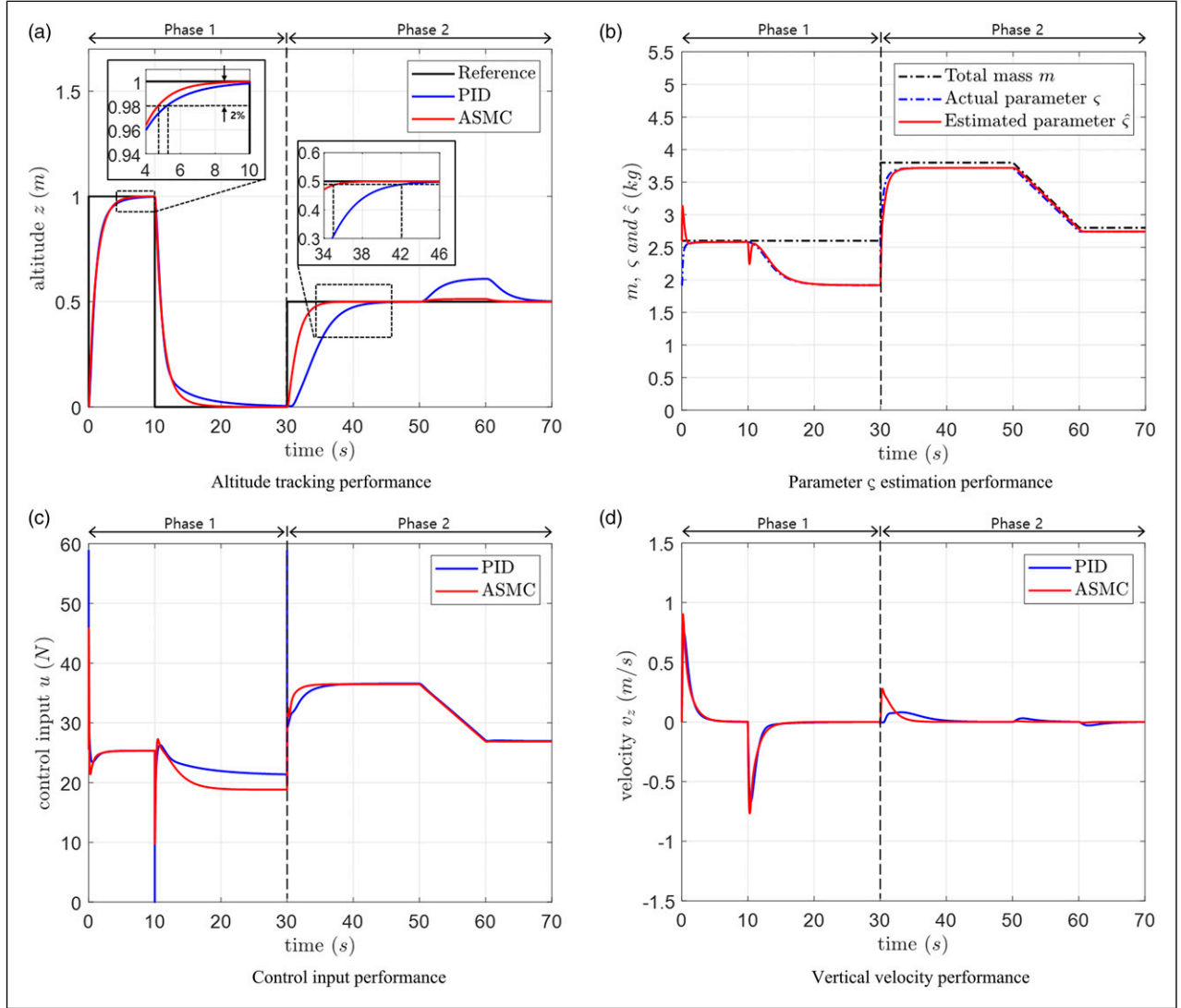


**Figure 5.** Performance comparisons between our new controller (ASMC) and a conventional PID controller (PID) with the ground effect only ( $0s < t < 30s$ ) and with both the ground effect and a varying system mass ( $t > 30s$ ). (a) Altitude tracking performance; (b) parameter  $\zeta$  estimation performance; (c) control input performance; (d) vertical velocity performance.

controller 7.7 s to reach the altitude setpoint of 1.5 m while our ASMC only needs 4.8 s to complete the task. Furthermore, once we started to decrease the payload at  $t = 40$  s, the altitude tracking performance of the PID controller deteriorates considerably as the vehicle significantly drifts away from the altitude setpoint. With the PID controller, it took the quadcopter about 17 s to return to the correct altitude, that is, at  $t = 57$  s when the water had all been emptied and the payload was constant again. Meanwhile, with the proposed adaptation law our ASMC exhibits a very robust performance and keeps the desired altitude despite the system mass variation (Figure 4(b)). The control input (Figure 4(c)) and vertical velocity (Figure 4(d)) also demonstrate that the velocity performance of the new controller is superior throughout the duration of the simulation.

**4.2.2. Altitude tracking flight under mass variation and ground effect.** This simulation scenario focuses on providing observations of the system control performance in the presence of a varying system mass and the ground effect. We again split this simulation into two phases: (1) The vehicle takes off, climbs, and lands with the ground effect but without system mass variation, and (2) the vehicle takes off, climbs, and maintains an altitude of 0.5 m feeling the ground effect and also a mass variation (Figure 5(a)). It should be noted that the controller gains are the same as in the previous scenario.

Phase 1 covers the time from  $t = 0$  to 30 s. During the early stage of this phase, the vehicle takes off and climbs to an altitude setpoint of 1 m. The expectation is that it should exhibit a similar performance as during Phase 1 of the

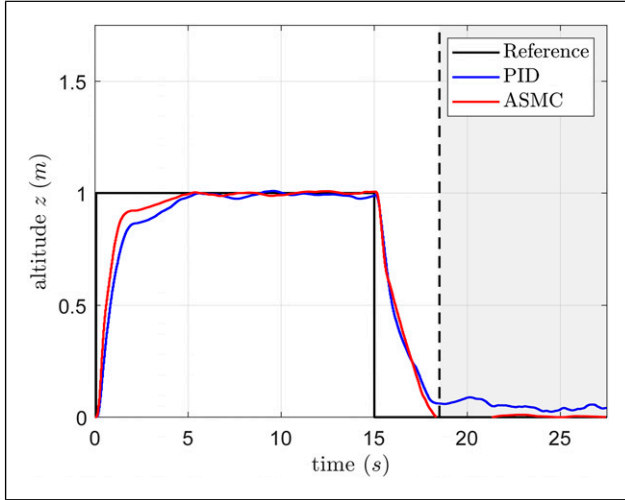


**Figure 6.** Comparison of altitude tracking performance between our controller (ASMC) and a conventional PID controller (PID) in experimental Scenario 1.

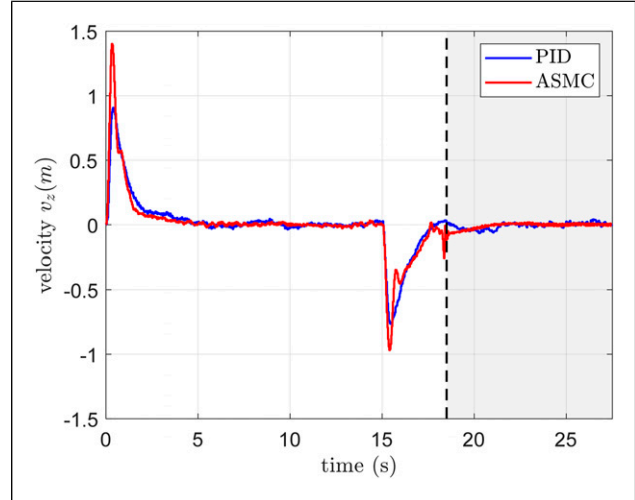


**Figure 8.** Comparison of vertical velocity performance between our controller (ASMC) and a conventional PID controller (PID) in experimental Scenario 1.

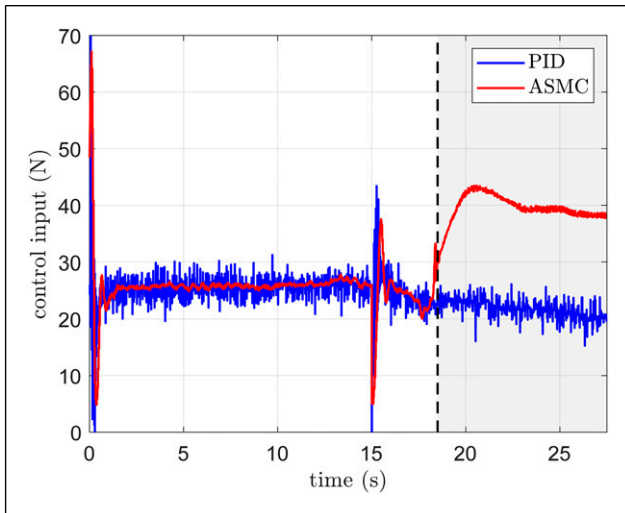


**Figure 7.** Comparison of control input between our controller (ASMC) and a conventional PID controller (PID) in experimental Scenario 1.

previous scenario (Figure 4). However, this time only our controller was capable to drive the vehicle to its setpoint within the expected settling time of about 4.7 s; the PID controller took about 5.5 s (Figure 8). Furthermore, the robustness of our controller against the ground effect can be seen more clearly during the later stage of this phase (between  $t = 10$  to 30 s) when the quadcopter is supposed to land. While our ASMC takes 9 s, the PID controller needs 16 s to complete the task.

At the beginning of Phase 2 ( $t = 30$  s), a payload of 1.2 kg is attached to the vehicle. We test the robustness of our ASMC controller by conducting a low-altitude flight at 0.5 m. Clearly, and despite the increasing influence of the

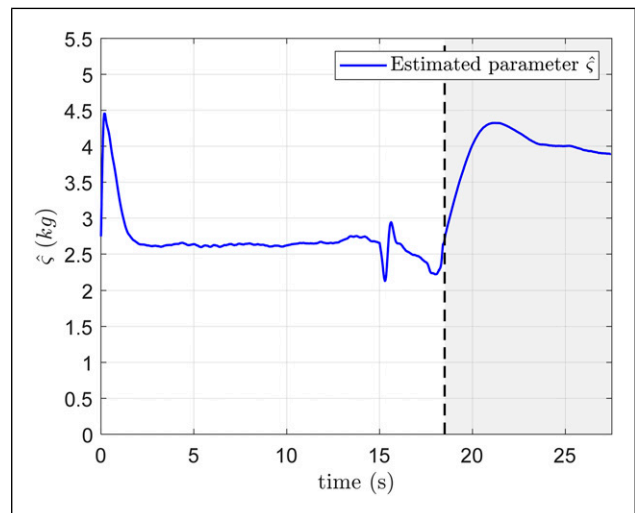


**Figure 9.** Parameter  $\hat{\zeta}$  in experimental Scenario 1.

ground effect, our ASMC controller exhibits a superior performance only requiring a settling time of about 5 s versus 11.5 s for the PID controller (see insets in Figure 8). The comparison between the total mass, the actual and estimated values of  $\zeta$  (Figure 5(b)), the control input performance (Figure 5(c)), and the vertical velocity response (Figure 5(d)) also demonstrate the effectiveness of the proposed method.

### 4.3. Experimental results and discussions

In this subsection, we present the experimental results. In order to verify the validity of the simulation results presented in the previous subsection, we also divided the experiment into two scenarios, namely Scenario 1, consisting of a landing task without mass variation, and



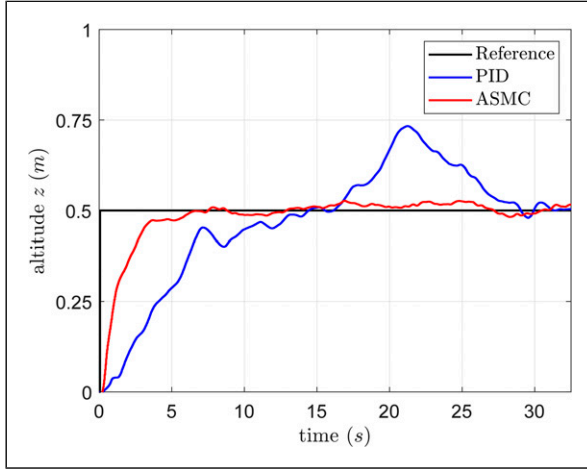


**Figure 10.** Comparison of altitude tracking performance between our controller (ASMC) and a conventional PID controller (PID) in experimental Scenario 2.

Scenario 2, consisting of altitude tracking flights with mass variation. Videos of the experiment can be found at <https://youtu.be/9p7oF7B6Hao>.

**4.3.1. Landing task without mass variation.** In Scenario 1, the quadcopter (Figure 2(a)) takes off from the ground, climbs to an altitude of 1 m, and is supposed to maintain this altitude for a few seconds before landing (Figure 6). The responses of the two controllers are similar between  $t = 0$  to  $t = 15$  s. Clearly, both controllers are capable to track the reference setpoint of 1 m. However, later on (between  $t = 15$  and 27 s), when the vehicle lands, our controller exhibits a remarkable robustness against the ground effect and quickly lands the quadcopter, completing the task at  $t = 18.5$  s (gray part in Figure 6). In contrast, the PID controlled quadcopter exhibits a rather fluctuating and sliding flight path near the ground.

The control input (Figure 7) and vertical velocity performance (Figure 8) also demonstrate that our controller works well due to the adaptive law. The estimated parameter value  $\hat{\zeta}$  decreases when the quadcopter is close to the ground ( $t = 16$  to 18.5 s, Figure 9), which is due to the increase in thrust due to the ground effect. This decrease appears to have the quadcopter lands fully.

**4.3.2. Altitude tracking flights with mass variation.** In Scenario 2, the vehicle has to maintain a low altitude (0.5 m) while the system mass is varying. The quadcopter (Figure 2(b)) takes off with an extra payload of 1.2 kg (1 kg of water and a pump weighing 0.2 kg), and its total mass gradually decreases at a rate of about 0.1 kg/s (from  $t = 15$  s onwards) until all of the water is discharged (by the pump). Early in this scenario ( $t = 0$  to 15 s) when the vehicle takes off and climbs to reach the setpoint of 0.5 m, our controller completes this task much faster than the PID controller in terms of rising time and settling time (Figure 10). Later on

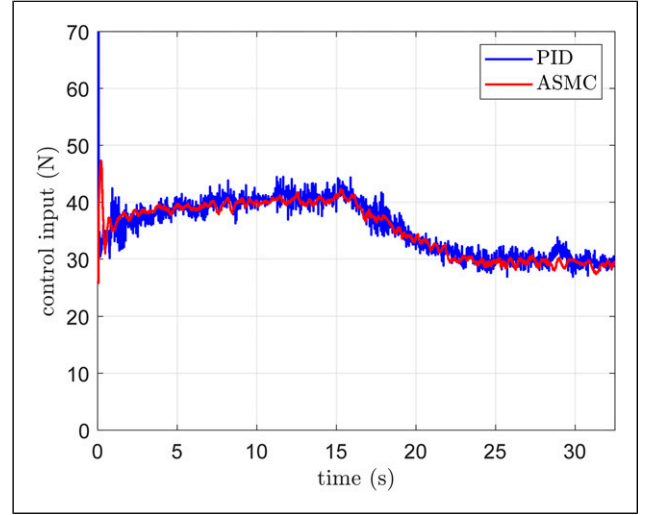


**Figure 11.** Comparison of control input between our controller (ASMC) and a conventional PID controller (PID) in experimental Scenario 2.

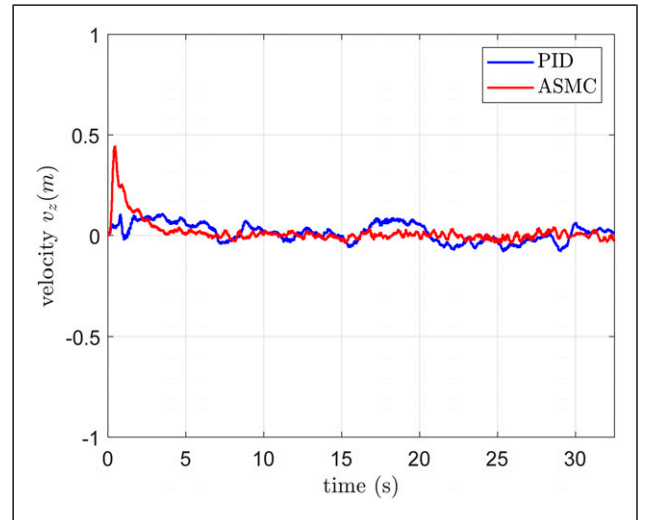


**Figure 12.** Comparison of vertical velocity between our controller (ASMC) and a conventional PID controller (PID) in experimental Scenario 2.

( $t = 15$  to 32 s), when the system mass decreases, our controller is capable of maintaining the vehicle's altitude (tracking errors below 0.2 m) while the PID controller fails. The unsatisfactory performance of the PID controller can be explained by its design, which only considers the nominal mass; that is, it is incapable of dealing with mass variations.

The control input (Figure 11) and vertical velocity performance (Figure 12) also demonstrate the superiority of our method for handling system mass variations. The estimated value  $\hat{\zeta}$  yields an accurate and stable reflection of the system's actual mass change (Figure 13). We should point out that between  $t = 0$  to 2 s, the estimated value increases (from 2.6 kg to 4 kg), while from  $t = 15$  to 25 s, the

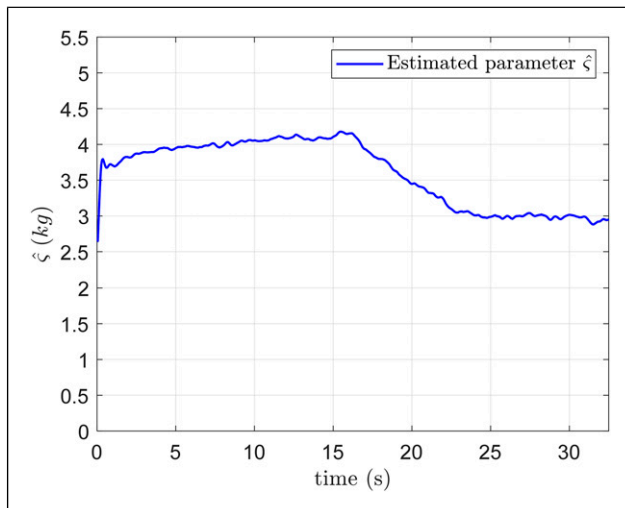


**Figure 13.** Estimated uncertain parameter in experimental Scenario 2.

estimated value decreases (from 4 kg to 3 kg), reflecting the changes in the actual parameters.

In summary, our proposed controller is capable of delivering superior altitude control performance even in the presence of strong system mass variations and the ground effect. It clearly outperformed the conventional PID controller which hold much promise for a wide range of future quadcopter applications, especially given the relatively straightforward design procedure of the new controller.

## 5. Conclusions

This paper presented an adaptive control algorithm for the quadcopter altitude tracking control problem in the presence of both ground effect and varying payload. We derived the controller using the sliding mode control technique and Lyapunov stability theory, and were able to strictly prove its validity. Results from both the simulations and experiments involving several scenarios clearly demonstrated the effectiveness of our controller. The merit of this work is scalable as it can be applied to several real-world quadcopter applications that are operated under system mass variation at low altitudes and require a high-performance controller, for example, precision docking, auto-charging systems, auto-delivery services, agricultural, and/or fire-fighting quadcopters. Finally, the validity of the proposed algorithms was verified by experimentally demonstrating its improved altitude tracking performance. In the future, we will work on the application of this approach to an agricultural spraying quadcopter system.

## Acknowledgments

This research was supported by the MSIT (Ministry of Science and ICT), Korea, under the ITRC (Information Technology Research Center) support program (IITP-2021-2018-0-01423) supervised by the IITP (Institute for Information & Communications Technology Planning & Evaluation).

## Declaration of conflicting interests

The author(s) declared no potential conflicts of interest with respect to the research, authorship, and/or publication of this article.

## Funding

The author(s) disclosed receipt of the following financial support for the research, authorship, and/or publication of this article: This research was supported by the Basic Science Research Program through the National Research Foundation of Korea (NRF) funded by the Ministry of Education (2020R1A6A1A03038540).

## ORCID iDs

Ji-Won Lee  <https://orcid.org/0000-0002-6650-9753>

Nguyen Xuan-Mung  <https://orcid.org/0000-0001-5632-9399>

## References

- Alexis K, Nikolakopoulos G, Tzes A, et al. (2009) Coordination of helicopter UAVs for aerial forest-fire surveillance. In: Valavanis KP (ed) *Applications of Intelligent Control to Engineering Systems*. Dordrecht: Springer Netherlands, 169–193.
- Besnard L, Shtessel YB and Landrum B (2012) Quadrotor vehicle control via sliding mode controller driven by sliding mode disturbance observer. *Journal of the Franklin Institute* 349(2): 658–684.
- Cho H, Udvardi FE and Wanichanon T (2020) Autonomous precision control of satellite formation flight under unknown time-varying model and environmental uncertainties. *The Journal of the Astronautical Sciences* 67(4): 1470–1499.
- DanJun L, Yan Z, Zongying S, et al. (2015) Autonomous landing of quadrotor based on ground effect modelling. In: 2015 34th Chinese control conference (CCC), 28–30 July 2015, Hangzhou, China, pp. 5647–5652.
- Das A, Lewis F and Subbarao K (2009) Backstepping approach for controlling a quadrotor using lagrange form dynamics. *J Intell Robot Syst* 56(1): 127–151.
- Dong W, Gu G-Y, Zhu X, et al. (2014) High-performance trajectory tracking control of a quadrotor with disturbance observer. *Sensors and Actuators A: Physical* 211: 67–77.
- Elmokadem T (2019) Distributed coverage control of quadrotor multi-UAV systems for precision agriculture. *IFAC-PapersOnLine* 52(30): 251–256.
- Gao G and Wang J (2013) Reference command tracking control for an air-breathing hypersonic vehicle with parametric uncertainties. *Journal of the Franklin Institute* 350(5): 1155–1188.
- Goodarzi FA, Lee D and Lee T (2015) Geometric control of a quadrotor UAV transporting a payload connected via flexible cable. *International Journal of Control, Automation and Systems* 13(6): 1486–1498.
- Hassan K (2002) *Nonlinear Systems*. 3rd edition. Upper Saddle River, NJ, USA: Prentice Hall.
- Hua C, Chen J and Guan X (2018) Adaptive prescribed performance control of QAVs with unknown time-varying payload and wind gust disturbance. *Journal of the Franklin Institute* 355(14): 6323–6338.
- Hua MD, Hamel T, Morin P, et al. (2009) A control approach for thrust-propelled underactuated vehicles and its application to

- VTOL drones. *IEEE Transactions on Automatic Control* 54(8): 1837–1853.
- Jia Z, Yu J, Mei Y, et al. (2017) Integral backstepping sliding mode control for quadrotor helicopter under external uncertain disturbances. *Aerospace Science and Technology* 68: 299–307.
- Kim J, Kang M-S and Park S (2009) Accurate modeling and robust hovering control for a quad-rotor VTOL aircraft. In: Selected papers from the 2nd International Symposium on UAVs, Reno, Nevada, U.S.A, June 8–10, 2009 (eds Valavanis KP, Beard R, Oh P, et al.), pp. 9–26. Dordrecht: Springer Netherlands.
- Lee B-Y, Hong S-M, Yoo D-W, et al. (2015) Design of a neural network controller for a slung-load system lifted by 1 quad-rotor. *Journal of Automation and Control Engineering* 3(1): 9–14.
- Lee D, Jin Kim H and Sastry S (2009) Feedback linearization versus adaptive sliding mode control for a quadrotor helicopter. *International Journal of Control, Automation and Systems* 7(3): 419–428.
- Liu Z, Liu X, Chen J, et al. (2019) Altitude control for variable load quadrotor via learning rate based robust sliding mode controller. *IEEE Access* 7: 9736–9744.
- Mahony R, Kumar V and Corke P (2012) Multirotor aerial vehicles: modeling, estimation, and control of quadrotor. *IEEE Robotics & Automation Magazine* 19(3): 20–32.
- Muñoz F, González-Hernández I, Salazar S, et al. (2017) Second order sliding mode controllers for altitude control of a quadrotor UAS: real-time implementation in outdoor environments. *Neurocomputing* 233: 61–71.
- Nguyen NP and Hong SK (2019) Fault diagnosis and fault-tolerant control scheme for quadcopter UAVs with a total loss of actuator. *Energies* 12(6): 1139.
- Pham TH, Ichalal D and Mammar S (2019) LPV and nonlinear-based control of an autonomous quadcopter under variations of mass and moment of inertia. *IFAC-PapersOnLine* 52(28): 176–183.
- Qiao J, Liu Z and Zhang YZ (2018) Gain scheduling based PID control approaches for path tracking and fault tolerant control of a quad-rotor UAV. *International Journal of Mechanical Engineering and Robotics Research* 7(4): 401–408.
- Ramirez-Rodriguez H, Parra-Vega V, Sanchez-Orta A, et al. (2014) Robust backstepping control based on integral sliding modes for tracking of quadrotors. *J Intell Robot Syst* 73(1): 51–66.
- Rodríguez-Mata AE, Flores G, Martínez-Vásquez AH, et al. (2018) Discontinuous high-gain observer in a robust control UAV quadrotor: real-time application for watershed monitoring. *Mathematical Problems in Engineering* 2018(2): 1–10.
- Rubio Hervas J and Reyhanoglu M (2014) Thrust-vector control of a three-axis stabilized upper-stage rocket with fuel slosh dynamics. *Acta Astronautica* 98: 120–127.
- Sadeghzadeh I, Abdolhosseini M and Zhang Y (2014) Payload drop application using an unmanned quadrotor helicopter based on gain-scheduled PID and model predictive control. *Un. Sys* 2(1): 39–52.
- Sanchez-Cuevas P, Heredia G and Ollero A (2017) Characterization of the aerodynamic ground effect and its influence in multirotor control. *International Journal of Aerospace Engineering* 2017: 1–17.
- Sankaranarayanan VN and Roy S (2018) Introducing switched adaptive control for quadrotors for vertical operations. *Optimal Control Applications and Methods* 41: 1875–1888.
- Sierra JE and Santos M (2019) Wind and payload disturbance rejection control based on adaptive neural estimators: application on quadrotors. *Complexity* 2019(1): 1–20.
- Wei G, Wang Z, Li W, et al. (2014) A survey on gain-scheduled control and filtering for parameter-varying systems. *Discrete Dynamics in Nature and Society* 2014: 1–10.
- Xuan-Mung N and Hong SK (2019) Robust backstepping trajectory tracking control of a quadrotor with input saturation via extended state observer. *Applied Sciences* 9(23): 5184.
- Xuan-Mung N, Hong SK, Nguyen NP, et al. (2020) Autonomous quadcopter precision landing onto a heaving platform: new method and experiment. *IEEE Access* 8: 167192–167202.
- Zhang X, Li X, Wang K, et al. (2014) A survey of modelling and identification of quadrotor robot. *Abstract and Applied Analysis* 2014: 320526.
- Zhang Y, Chen Z, Zhang X, et al. (2018) A novel control scheme for quadrotor UAV based upon active disturbance rejection control. *Aerospace Science and Technology* 79: 601–609.